XL CILAMCE
IBERO-LATIN AMERICAN CONGRESS ON COMPUTATIONAL METHODS IN ENGINEERING
NOVEMBER 11-14, 2019
Praiamar Natal Hotel & Convention
Natal, RN-BRAZIL

NUMERICAL MODELING OF VISCOELASTIC BIDIMENSIONAL PROBLEMS USING MESHLESS LOCAL PETROV-GALERKIN METHOD

Catarina de Nazaré P. Pinheiro
José Antônio F. Santiago
José Claudio de F. Telles
catarina.pinheiro@coc.ufrj.br
santiago@coc.ufrj.br
telles@coc.ufrj.br
Federal University of Rio de Janeiro
Centro de Tecnologia - Bloco B, Sala 101 - Ilha do Fundão, 21941-909, Rio de Janeiro/RJ, Brazil

Abstract. In engineering studies, most of the existing phenomena are modeled by differential and integral equations. The analysis of the behavior of these systems can be performed through analytical or numerical methods, the latter which presents an approximate approach to the results. Due to the complexity of the real-life structure models, the use of approximate solutions is increasing.Among these solutions, the Meshless methods are the most recent and have as advantage over those without of mesh, making easy the refinement where existing more complexity of the behaviors variables. However, because they are relatively recent methods, the use of these solutions is not still enough to research and to apply in real structures. Viscoelastic materials are defined as presenting a combination of elastic and viscous elements. A viscoelastic structure is represented by physical models that increase the number of elements as the complexity of the problem grows. Therefore, for more complex models,it is necessary to use numerical solutions. In this context, the purpose of this paper is the application of the Meshless Local Petrov-Galerkin 01 (MLPG-01) and MLPG-02 or Local Collocation Method to study two-dimensional viscoelastic structures, subjected to in-plane state, in order to perform an analysis of the effectiveness and convergence of each method evaluated, thus verifying its efficiency for these structures.

Keywords: Local Petrov-Galerkin Method, Collocation Method, Viscoelasticity.

1 Introduction

The recent development of structural project, in general, is directly related to improvement of the physical theories represented by means of mathematical models. Hence, partial differential equations for mathematical formulation of problems involving one or more independent variables, can be deeply studied to employed in several engineering fields [1].

The use of problem domain with more complex geometries and materials has been discovered in engineering, more challenges arise in the area of computational mechanics [2]. In the past, the behavior of some materials has been simplified. Nowadays it is modeled in detail, as in the case of viscoelastic materials. These materials are defined by models made from the combination of elastic and viscous elements [3], and present, in general, high complexity, restricting the obtaining of their analytical solution.

Technological advancement has enabled more complex problems with more accurate results through the use of appropriate numerical solutions. Among these, the meshless methods have been presented as a viable alternative due to their flexibility and reduction of the human labor for mesh discretization. [4]

Meshless methods are defined as numerical methods for boundary value problem (BVP) solving, which establish a system of algebraic equations for solving these problems, independent of a mesh definition [5]. The main features of these methods are the construction of a function of their own, and the absence of nodal connectivity that facilitates domain discretization.

Among the meshless methods developed so far are the Local Collocation method or Meshless Local Petrov-Galerkin 02 (MLPG-02) and Meshless Local Petrov-Galerkin 01. Both methods use a local approach to the problem. The collocation method, however, makes use of the strong formulation in its development, that is the differential equation itself, while the local Petrov-Galerkin method uses the weak formulation of the problem.

The local Petrov-Galerkin method has six best-known variations that are distinguished by the type of weak formulation employed and the test function applied. The work of Atluri and Shen [6] shows the main differences of each variation. In this paper we used variation 01 is employed, in which the test function for each local subdomain used was the weight function derived from the moving least squares method, and variation 02 of the method, in which the test function for each local subdomain used was the Dirac‘s Delta function. Thus, the collocation method can be treated as special case of the MLPG approach. [4]

Thus, the goal of this work is the analysis of the collocation method and local method of Petrov-Galerkin applied to quasi-static linear viscoelastic problems submitted to the plane stress state, with the verification of the relative and comparative errors between the methods.

2 Basic Viscoelasticity Equations

It is considered a quasi-static linear viscoelastic homogeneous solid body with domain Ω under a Γ boundary. This body can be described through equilibrium equations, which relate acting forces to internal stresses, strain-displacement relations, and the constitutive equation, which relates stresses to acting deformations.

The boundary conditions in the body are described as:

$$u_i\left(\mathbf{x},\mathrm{t}\right) = \overline{u}_i\left(\mathbf{x},\mathrm{t}\right), \qquad \text{in } \Gamma_u, \tag{1}$$

$$t_i\left(\mathbf{x},\mathrm{t}\right) = \sigma_{ij}\left(\mathbf{x},\mathrm{t}\right) n_j\left(\mathbf{x}\right) = \overline{t}_i\left(\mathbf{x},\mathrm{t}\right), \qquad \text{in } \Gamma_t. \tag{2}$$

The equilibrium relations are represented in the index form as:

$$\sigma_{ij,j}\left(\mathbf{x},\mathrm{t}\right) + b_i\left(\mathbf{x},\mathrm{t}\right) = 0. \tag{3}$$

The deformation-displacement relations:

$$\varepsilon_{ij} = \frac{1}{2}\left(u_{i,j} + u_{j,i}\right). \tag{4}$$

And the constitutive law are obtained, in this study, through the three-parameter solid model. In the creep phase, for a constant stress $\sigma = \sigma_0 \mathrm{H}(t)$, where $\mathrm{H}(t)$ represents the Heaviside function, the strain is calculated as:

$$\varepsilon(t) = \sigma_0 J(t). \tag{5}$$

where $J(t)$ is the creep function.

The creep function for the three-parameter solid model is represented according to Flügge [3] by:

$$\frac{p_1}{q_1} e^{-\lambda t} + \frac{1}{q_0}\left(1 - e^{-\lambda t}\right) \tag{6}$$

where:

$$\lambda = \frac{q_0}{q_1}, \qquad p_1 = \frac{F}{E_1 + E_2}, \qquad q_0 = \frac{E_1 E_2}{E_1 + E_2}, \qquad q_1 = \frac{E_1 F}{E_1 + E_2}. \tag{7}$$

with E_1, E_2 being the modulus of elasticity of the material, and F being the viscosity constant of the model.

For the development of constitutive law of a three-dimensional viscoelasticity model , it is useful to decompose the stress tensor $\boldsymbol{\tau}$, which describes the tensional state of a body, in two parts, the hydrostatic $\boldsymbol{\tau}^s$ and the deviatoric $\boldsymbol{\tau}^d$ [7], represented by:

$$\boldsymbol{\tau} = \boldsymbol{\tau}^s + \boldsymbol{\tau}^d. \tag{8}$$

The hydrostatic tensor in an isotropic infinitesimal element is related to the volume variation with the constant form [7], and has the following configuration:

$$\boldsymbol{\tau}^s = \begin{bmatrix} \sigma_0 & 0 & 0 \\ 0 & \sigma_0 & 0 \\ 0 & 0 & \sigma_0 \end{bmatrix}, \tag{9}$$

where σ_0 is calculated as:

$$\sigma_0 = \frac{1}{3}\left(\sigma_\mathrm{x} + \sigma_\mathrm{y} + \sigma_\mathrm{z}\right). \tag{10}$$

For small deformations, the stress deviator, in the same element, is associated with the shape change without volume variation, that is, the distortion of the element. This tensor is represented by:

$$\boldsymbol{\tau}^d = \begin{bmatrix} \sigma_\mathrm{x} - \sigma_0 & \tau_\mathrm{xy} & \tau_\mathrm{xz} \\ \tau_\mathrm{yx} & \sigma_\mathrm{y} - \sigma_0 & \tau_\mathrm{yz} \\ \tau_\mathrm{zx} & \tau_\mathrm{zy} & \sigma_\mathrm{z} - \sigma_0 \end{bmatrix}. \tag{11}$$

Each stress portion is associated with a strain. The deformation regarding the hydrostatic tensor is presented as:

$$\boldsymbol{\varepsilon}^s = \begin{bmatrix} \varepsilon_{\mathrm{v}} & 0 & 0 \\ 0 & \varepsilon_{\mathrm{v}} & 0 \\ 0 & 0 & \varepsilon_{\mathrm{v}} \end{bmatrix}, \tag{12}$$

where ε_{v} is calculated as:

$$\varepsilon_{\mathrm{v}} = \frac{1}{3}\left(\varepsilon_{\mathrm{x}} + \varepsilon_{\mathrm{y}} + \varepsilon_{\mathrm{z}}\right). \tag{13}$$

The deviatoric strain portion is represented by:

$$\boldsymbol{\varepsilon}^d = \begin{bmatrix} \varepsilon_{\mathrm{x}} - \varepsilon_{\mathrm{v}} & \frac{1}{2}\gamma_{\mathrm{xy}} & \frac{1}{2}\gamma_{\mathrm{xz}} \\ \frac{1}{2}\gamma_{\mathrm{yx}} & \varepsilon_{\mathrm{y}} - \varepsilon_{\mathrm{v}} & \frac{1}{2}\gamma_{\mathrm{yz}} \\ \frac{1}{2}\gamma_{\mathrm{zx}} & \frac{1}{2}\gamma_{\mathrm{zy}} & \varepsilon_{\mathrm{z}} - \varepsilon_{\mathrm{v}} \end{bmatrix}. \tag{14}$$

Thus, the constitutive equations can be represented as a function of hydrostatic and deviatoric stresses as:

$$\boldsymbol{\varepsilon}^d = J_1(t)\boldsymbol{\tau}^d, \tag{15}$$

$$\boldsymbol{\varepsilon}^s = J_2(t)\boldsymbol{\tau}^s, \tag{16}$$

where $J_1(t)$ is the creep function of equation (6) and

$$J_2(t) = \frac{1}{3K}, \tag{17}$$

with K being the volumetric expansion module, represented by:

$$K = \frac{E}{3\left(1 - 2\nu\right)}. \tag{18}$$

3 Meshless Method

When constructing the approximate solution of a meshless method, generally, a linear combination of allowable or approximation functions is adopted. In this case, the approximate function, according to Nguyen et al. [8], is represented by

$$u^h\left(\mathbf{x}\right) = \sum_{i=1}^{n} \phi_i\left(\mathbf{x}\right)\hat{u}_i = \boldsymbol{\Phi}^T\left(\mathbf{x}\right)\mathbf{u}. \tag{19}$$

One of the most general techniques for solving boundary value problems is the use of the weighted residuals method. The idea of this method is the construction of an approximate solution that satisfies the presented differential equation and the boundary conditions imposed according to a certain approximation error criterion.

This approximate function generally does not initially satisfy the value of the actual function, generating a residue represented by

$$R\left(\mathbf{x}\right) = \mathcal{L}u^h\left(\mathbf{x}\right) - f\left(\mathbf{x}\right). \tag{20}$$

Where $\mathcal{L}$ is the differential operator applied to the problem under analysis and $f\left(\mathbf{x}\right)$ is the value of the analytic function.

In order for the approximate solution to be the same as the analytical one, the residue value should be minimized. In the weighted residual method, this minimization is done by requiring that the internal product of the residue with a set of test fuctions $\mathbf{\Psi}$ equals zero, as shown below.

$$\int_{\Omega} \mathbf{\Psi} \left(\mathcal{L} u^h \left(\mathbf{x} \right) - f \left(\mathbf{x} \right) \right) d\Omega = 0. \tag{21}$$

The approximate function u^h can be replaced by the equation Eq. (19) resulting in:

$$\int_{\Omega} \mathbf{\Psi} \left(\mathcal{L} \mathbf{\Phi}^T \left(\mathbf{x} \right) \mathbf{u} - f \left(\mathbf{x} \right) \right) d\Omega = 0. \tag{22}$$

The test function varies according to the meshless method adopted. The approximation functions for meshless methods, in turn, are constructed from three items: A compact support weight function, a set of position-dependent coefficients, and a polynomial base. In this study, the function used was the moving least squares approximation.

4 Moving Least Square

A function $u \left(\mathbf{x} \right)$ named as $u^h \left(\mathbf{x} \right)$, in the domain Ω, is made up of a sum of linearly independent functions in the same domain, in such way that:

$$u^h \left(\mathbf{x} \right) = \mathbf{p}^T \left(\mathbf{x} \right) \mathbf{a} \left(\mathbf{x} \right), \qquad \forall \, \mathbf{x} \in \Omega_{\mathrm{x}}, \tag{23}$$

where:

$\mathbf{p}^T \left(\mathbf{x} \right)$is the transposed vector containing a complete polynomial basis of m terms, given by:

$$\mathbf{p}^T \left(\mathbf{x} \right) = \begin{bmatrix} 1 & \mathbf{x} & \mathbf{x}^2 & \dots & \mathbf{x}^m \end{bmatrix}. \tag{24}$$

$\mathbf{a} \left(\mathbf{x} \right)$ is the vector of coefficients to be determined, which depends on the position of x, given by:

$$\mathbf{a}^T \left(\mathbf{x} \right) = \begin{bmatrix} \mathrm{a}_0(\mathbf{x}) & \mathrm{a}_1(\mathbf{x}) & \mathrm{a}_2(\mathbf{x}) & \dots & \mathrm{a}_{\mathrm{m}}(\mathbf{x}) \end{bmatrix}. \tag{25}$$

For the quadratic basis in two-dimensional problems (m = 6), the value of $\mathbf{p}^T \left(\mathbf{x} \right) = \begin{bmatrix} 1 & \mathrm{x} & \mathrm{y} & \mathrm{x}^2 & \mathrm{y}^2 & \mathrm{xy} \end{bmatrix}$.

To determine the coefficient vector $\mathbf{a} \left(\mathbf{x} \right)$ the quadratic residual function $J \left(\mathbf{x} \right)$ is calculated, defined as:

$$J = \sum_{i=1}^{n} w_i \left(\mathbf{x} - \mathbf{x}_i \right) \left[u^h \left(\mathbf{x}_i, \mathbf{x} \right) - \hat{u}_i \right]^2,$$

$$J = \sum_{i=1}^{n} w_i \left(\mathbf{x} - \mathbf{x}_i \right) \left[\mathbf{p}^T \left(\mathbf{x}_i \right) \mathbf{a} \left(\mathbf{x} \right) - \hat{u}_i \right]^2, \tag{26}$$

where $w_i(\mathbf{x})$ is the weight function that assumes nonzero values only within its support, and depends on the position $\mathbf{x}$.

This equation can be written in matrix form as

$$J = \left[\mathbf{P} \mathbf{a} \left(\mathbf{x} \right) - \mathbf{u} \right]^T \mathbf{W} \left(\mathbf{x} \right) \left[\mathbf{P} \mathbf{a} \left(\mathbf{x} \right) - \mathbf{u} \right]. \tag{27}$$

where:

$$\mathbf{u}^T = \begin{bmatrix} u_1 & u_2 & \dots & u_{\mathrm{n}} \end{bmatrix}, \tag{28}$$

$$\mathbf{P} = \begin{bmatrix} p_1(\mathbf{x}_1) & p_2(\mathbf{x}_1) & \dots & p_{\mathrm{m}}(\mathbf{x}_1) \\ p_1(\mathbf{x}_2) & p_2(\mathbf{x}_2) & \dots & p_{\mathrm{m}}(\mathbf{x}_2) \\ \vdots & \vdots & \ddots & \vdots \\ p_1(\mathbf{x}_n) & p_2(\mathbf{x}_n) & \dots & p_{\mathrm{m}}(\mathbf{x}_n) \end{bmatrix}, \tag{29}$$

$$\mathbf{W}(\mathbf{x}) = \begin{bmatrix} w(\mathbf{x}-\mathbf{x}_1) & 0 & \dots & 0 \\ 0 & w(\mathbf{x}-\mathbf{x}_2) & \dots & 0 \\ \vdots & \vdots & \ddots & \vdots \\ 0 & 0 & \dots & w(\mathbf{x}-\mathbf{x}_n) \end{bmatrix}. \tag{30}$$

In order to obtain the best approximation, the functional J is minimized through its derivative in relation to the vector $\mathbf{a}$

$$\frac{\partial J}{\partial a} = \frac{\partial}{\partial a}\left[\left[\mathbf{P}\mathbf{a}(\mathbf{x}) - \mathbf{u}\right]^T \mathbf{W}(\mathbf{x}) \left[\mathbf{P}\mathbf{a}(\mathbf{x}) - \mathbf{u}\right]\right] = 0. \tag{31}$$

Resulting the set of m equations, described in vector notation as:

$$\mathbf{P}^T\mathbf{W}(\mathbf{x})\,\mathbf{P}\mathbf{a}(\mathbf{x}) = \mathbf{P}^T\mathbf{W}(\mathbf{x})\,\mathbf{P}\overline{\mathbf{u}}. \tag{32}$$

Written in simplified form as:

$$\mathbf{A}(\mathbf{x})\,\mathbf{a}(\mathbf{x}) = \mathbf{B}(\mathbf{x})\,\overline{\mathbf{u}}, \tag{33}$$

where A and B are arrays defined as:

$$\mathbf{B}(\mathbf{x}) = \mathbf{P}^T\mathbf{W}(\mathbf{x}), \tag{34}$$

$$\mathbf{A}(\mathbf{x}) = \mathbf{B}(\mathbf{x})\,\mathbf{P} = \mathbf{P}^T\mathbf{W}(\mathbf{x})\,\mathbf{P}. \tag{35}$$

Isolating the vector $\mathbf{a}(\mathbf{x})$, it is obtained:

$$\mathbf{a}(\mathbf{x}) = \mathbf{A}^{-1}(\mathbf{x})\,\mathbf{B}(\mathbf{x})\,\overline{\mathbf{u}}. \tag{36}$$

Substituting the value of $\mathbf{a}(\mathbf{x})$ into the equation Eq. (23), the result is the approximation by moving least squares, defined by:

$$u^h(\mathbf{x}) = \mathbf{p}^T(\mathbf{x})\mathbf{A}^{-1}(\mathbf{x})\,\mathbf{B}(\mathbf{x})\,\overline{\mathbf{u}}. \tag{37}$$

The interpolating function or shape function $\mathbf{\Phi}_i(\mathbf{x})$, associated with the ith node of point $\mathbf{x}$, therefore, is described as:

$$\mathbf{\Phi}_i(\mathbf{x}) = \mathbf{p}^T(\mathbf{x})\mathbf{A}^{-1}(\mathbf{x})\,\mathbf{B}(\mathbf{x}). \tag{38}$$

The moving least squares approximation is well defined when the matrix $\mathbf{A}$ is non-singular [4]. For this to occur, the number of minimum points within the local domain to be approximated must be greater than the number of terms in the polynomial basis $(n > m)$.

The smoothness of the shape function $\mathbf{\Phi_i}$ is determined by the smoothness of the base and the weight function [6]. For a smooth polynomial basis, the continuity of the function will be determined by its weight function. The function used in this study was Gaussian with radius, used by Atluri and Zhu [9] [10] with high accuracy results, defined as:

$$w_{\mathrm{i}}(\mathbf{x}) = \begin{cases} \dfrac{e^{-\left(\frac{d_i}{c}\right)^2} - e^{-\left(\frac{r_i}{c}\right)^2}}{1 - e^{-\left(\frac{r_i}{c}\right)^2}}, & \text{if } 0 \le d_{\mathrm{i}} \le r_{\mathrm{i}} \\ 0, & \text{if } d_{\mathrm{i}} \ge r_{\mathrm{i}} \end{cases} \tag{39}$$

where d_i is the distance from the point $\mathbf{x}_i$ to the point $\mathbf{x}$ and c is a constant representing the shape of the function defined as recommended by Belytschko [11].

5 Meshless Local Petrov-Galerkin 02 (MLPG-02) - Local Collocation Method

The meshless local Petrov-Galerkin 02 method uses the Dirac Delta function as its test function. In this case, applying the filtering property of the Dirac Delta function will result in the strong formulation in each node, that is, the equilibrium formulation itself. For nodes located in the problem domain this equation is represented by:

$$\sigma_{ij,j}\left(\mathbf{x},t\right) = -b_i\left(\mathbf{x},t\right). \tag{40}$$

For nodes located on the problem boundary, the formulation must meet the boundary conditions imposed in the equations Eq. (1) e Eq. (2).

In plane stress, the constitutive equation can be represented as a function of deviatoric and hydrostatic strain, in stress and strain vector form, as:

$$\boldsymbol{\sigma}\left(\mathbf{x},t\right) = \mathbf{D}_1 \begin{bmatrix} \varepsilon_v \\ \varepsilon_v \\ 0 \end{bmatrix} + \mathbf{D}_2 \begin{bmatrix} \varepsilon_x - \varepsilon_v \\ \varepsilon_y - \varepsilon_v \\ \frac{1}{2}\varepsilon_{xy} \end{bmatrix} \tag{41}$$

where

$$\mathbf{D}_1 = \begin{bmatrix} 3K & 0 & 0 \\ 0 & 3K & 0 \\ 0 & 0 & 3K \end{bmatrix}, \tag{42}$$

$$\mathbf{D}_2 = \begin{bmatrix} \frac{1}{J_1(t)} & 0 & 0 \\ 0 & \frac{1}{J_1(t)} & 0 \\ 0 & 0 & \frac{1}{J_1(t)} \end{bmatrix}. \tag{43}$$

Substituting the strain-displacement relationship in the constitutive equation gives:

$$\boldsymbol{\sigma}\left(\mathbf{x},t\right) = \mathbf{D}_1 \sum_{i=1}^{n} \mathbf{B}_1 \mathbf{u} + \mathbf{D}_2 \sum_{i=1}^{n} \mathbf{B}_2 \mathbf{u}. \tag{44}$$

where, for the plane state of stress, it is obtained:

$$\mathbf{B}_1 = \frac{1}{3KJ_1\left(t\right)+2} \begin{bmatrix} \phi_{,x} & \phi_{,y} \\ \phi_{,x} & \phi_{,y} \\ 0 & 0 \end{bmatrix}, \tag{45}$$

$$\mathbf{B}_2 = \begin{bmatrix} \beta_1\phi_{,x} & -\beta_2\phi_{,y} \\ -\beta_2\phi_{,x} & \beta_1\phi_{,y} \\ \frac{1}{2}\phi_{,y} & \frac{1}{2}\phi_{,x} \end{bmatrix}, \tag{46}$$

where:

$$\beta_1 = \frac{3KJ_1(t)+1}{3KJ_1(t)+2}, \tag{47}$$

$$\beta_2 = \frac{1}{3KJ_1(t)+2}. \tag{48}$$

Substituting into the equilibrium equation, the formulation of the local collocation method in terms of displacement is obtained in matrix form as:

$$\mathbf{L}^T\mathbf{D}_1\sum_{i=1}^{n}\mathbf{B}_1\mathbf{u} + \mathbf{L}^T\mathbf{D}_2\sum_{i=1}^{n}\mathbf{B}_2\mathbf{u} = -\mathbf{b}, \tag{49}$$

where:

$$\mathbf{L} = \begin{bmatrix} \frac{\partial}{\partial x} & 0 \\ 0 & \frac{\partial}{\partial y} \\ \frac{\partial}{\partial y} & \frac{\partial}{\partial x} \end{bmatrix}. \tag{50}$$

The traction vector $\bar{\mathbf{t}}(\mathbf{x},t)$ is described in terms of displacement as:

$$\bar{\mathbf{t}}(\mathbf{x},t) = \mathbf{N}(\mathbf{x})\mathbf{D}_1\sum_{i=1}^{n}\mathbf{B}_1\mathbf{u} + \mathbf{N}(\mathbf{x})\mathbf{D}_2\sum_{i=1}^{n}\mathbf{B}_2\mathbf{u}, \tag{51}$$

where

$$\mathbf{N}(\mathbf{x}) = \begin{bmatrix} n_x & 0 & n_y \\ 0 & n_y & n_x. \end{bmatrix}.$$

Thus, the boundary conditions in terms of displacement are described as

$$\mathbf{u}(\mathbf{x},t) = \overline{\mathbf{u}}(\mathbf{x},t), \qquad \text{em } \Gamma_u, \tag{52}$$

$$\mathbf{N}(\mathbf{x})\mathbf{D}_1\sum_{i=1}^{n}\mathbf{B}_1\mathbf{u} + \mathbf{N}(\mathbf{x})\mathbf{D}_2\sum_{i=1}^{n}\mathbf{B}_2\mathbf{u} = \bar{\mathbf{t}}(\mathbf{x},t), \qquad \text{em } \Gamma_t. \tag{53}$$

6 Meshless Local Petrov-Galerkin 01 Method (MLPG-01)

The local Petrov-Galerkin method makes use of weak formulation in a local subdomain belonging to the global domain. The local weak form of the equation Eq. (3) is described as

$$\int_{\Omega_s}\left[\sigma_{ij,j}(\mathbf{x},t) + b_i(\mathbf{x},t)\right]v_i(\mathbf{x})\,d\Omega_s = 0, \tag{54}$$

where $v_i(\mathbf{x})$ is the test function.

Using the property:

$$\sigma_{ij,j} v_i = \left(\sigma_{ij} v_i\right)_{,j} - \sigma_{ij} v_{i,j}. \tag{55}$$

And applying the divergence theorem in the equation Eq. (54) it is obtained:

$$\int_{\partial\Omega_s} \sigma_{ij}(\mathbf{x},t)\, n_j(\mathbf{x})\, v_i(\mathbf{x})\, d\Gamma - \int_{\Omega_s} \sigma_{ij}(\mathbf{x},t)\, v_{i,j}(\mathbf{x})\, d\Omega + \int_{\Omega_s} b_i(\mathbf{x},t)\, v_i(\mathbf{x})\, d\Omega = 0, \tag{56}$$

where $\partial\Omega_s$ is the boundary of the subdomain Ω_s. This boundary consists of three parts, $\partial\Omega_s = L_s \cup \Gamma_{su} \cup \Gamma_{st}$. the first component, L_s, corresponds to the boundary fully inserted in the global domain, Γ_{su} represents the boundary part $\partial\Omega_s$ pertaining to the prescribed global displacement boundary ($\Gamma_{su} = \partial\Omega_s \cap \Gamma_u$), and Γ_{su} is the portion referring to the intersection with the global boundary with prescribed forces ($\Gamma_{st} = \partial\Omega_s \cap \Gamma_t$).

The test function v_i to be used depends on the subtype of the local Petrov-Galerkin method. In this case, it was the Gaussian with radius function, given in the equation Eq. (39), seen as a weighting function in the moving least squares method, characteristic of the local Petrov-Galerkin 01 method.

Considering $t_i(\mathbf{x}) = \sigma_{ij}(\mathbf{x})\, n_j(\mathbf{x})$ and $\partial\Omega_s = L_s \cup \Gamma_{su} \cup \Gamma_{st}$, the equation Eq. (56) can be rewritten as:

$$\begin{aligned}\int_{L_s} t_i(\mathbf{x},t)\, v_i(\mathbf{x})\, d\Gamma + \int_{\Gamma_{su}} t_i(\mathbf{x},t)\, v_i(\mathbf{x})\, d\Gamma + \int_{\Gamma_{st}} t_i(\mathbf{x},t)\, v_i(\mathbf{x})\, d\Gamma \\ - \int_{\Omega_s} \sigma_{ij}(\mathbf{x},t)\, v_{i,j}(\mathbf{x})\, d\Omega + \int_{\Omega_s} b_i(\mathbf{x},t)\, v_i(\mathbf{x})\, d\Omega = 0.\end{aligned} \tag{57}$$

Due to the characteristic of the weighting function to zero when the value of the distance between the points is the radius itself, that is, at the end of the function, the boundary L_s is removed from the equation. Also, in the boundary Γ_{st} the value of $t_i(\mathbf{x})$ can be replaced by the equation Eq. (2). Substituting the values gives the general equation of the local method of Petrov-Galerkin 01 for viscoelasticity.

$$\begin{aligned}\int_{\Gamma_{su}} t_i(\mathbf{x},t)\, v_i(\mathbf{x})\, d\Gamma - \int_{\Omega_s} \sigma_{ij}(\mathbf{x},t)\, v_{i,j}(\mathbf{x})\, d\Omega = \\ \int_{\Omega_s} b_i(\mathbf{x},t)\, v_i(\mathbf{x})\, d\Omega + \int_{\Gamma_{st}} \bar{t}_i(\mathbf{x},t)\, v_i(\mathbf{x})\, d\Gamma.\end{aligned} \tag{58}$$

This equation is valid for points located in the domain and boundary Γ_{st}. In the boundary Γ_{su}, boundary conditions may be imposed separately through the direct integration method, similar to the Collocation method, or may be imposed within the equation. Eq. (58) with a penalty factor as shown in equation Eq. (59)

$$\begin{aligned}\int_{\Gamma_{su}} t_i(\mathbf{x},t)\, v_i(\mathbf{x})\, d\Gamma - \int_{\Omega_s} \sigma_{ij}(\mathbf{x},t)\, v_{i,j}(\mathbf{x})\, d\Omega - \alpha \int_{\Gamma_{su}} u_i(\mathbf{x},t)\, v_i(\mathbf{x})\, d\Gamma = \\ - \int_{\Omega_s} b_i(\mathbf{x},t)\, v_i(\mathbf{x})\, d\Omega + \int_{\Gamma_{st}} \bar{t}_i(\mathbf{x},t)\, v_i(\mathbf{x})\, d\Gamma - \alpha \int_{\Gamma_{su}} \overline{u}_i(\mathbf{x},t)\, v_i(\mathbf{x})\, d\Gamma.\end{aligned} \tag{59}$$

As in the Collocation method, the stress is replaced as a function of the displacement for the method implementation.

7 Linear viscoelasticity Time integration

The above methods have all been solved for problems with constant stress over time. For quasi-static problems of linear viscoelastic materials with time varying stress, an alternative solution is to use the integral formulation of the time domain problem. Based on the formulation given by Flügge [3],

the incremental method for three-dimensional linear viscoelasticity uses the concepts of deviatoric and hydrostatic tensor and hereditary integrals for its formulation.

In this case, the constitutive equation of the problem is represented as:

$$\boldsymbol{\varepsilon} = C_1\left(t-t'\right)\boldsymbol{\sigma}^s + C_2\left(t-t'\right)\boldsymbol{\sigma}^d, \tag{60}$$

where $C_1\left(t-t'\right)$ e $C_2\left(t-t'\right)$ are the creep functions referring to the hydrostatic and deviatoric portion.

The hereditary integral equations, seen in Flügge [3], can be described as a function of these two parts, considering the relaxation and creep functions applied only to the devitoric part. Thus this formulation can be broadly represented by:

$$\boldsymbol{\varepsilon}^s = \int_{\infty}^{t} C_1\left(t-t'\right)\frac{d\boldsymbol{\sigma}^s\left(t'\right)}{dt'}dt', \tag{61}$$

$$\boldsymbol{\varepsilon}^d = \int_{\infty}^{t} C_2\left(t-t'\right)\frac{d\boldsymbol{\sigma}^d\left(t'\right)}{dt'}dt'. \tag{62}$$

It is worth noting the elastic influence on the hydrostatic and viscoelastic portion in the deviatoric .

8 Numerical Examples

In this section two examples of two-dimensional viscoelastic solids subjected to the plane stress state with two distinct loads are solved.

8.1 Load History

For the development of the examples listed below, two loading histories were used, named C1 and C2 in this paper for historical didactic purposes.

Load history C1 represents a zero load to instant $t = 0^-$ and constant loading from the instant $t = 0^+$. This history is represented by a unit step function, as shown in figure Fig. 1 and mathematically expressed by:

$$P_{C1}\left(t\right) = Ph\left(t\right), \tag{63}$$

where:

P is the load applied to the structure;

$h\left(t\right)$ is the unit step function.

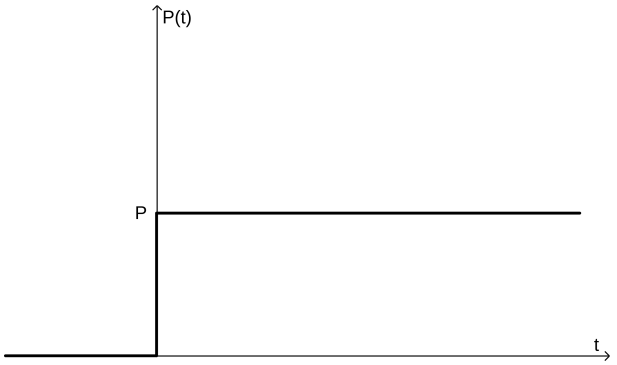

Figure 1. Load history C1

The load history C2 is represented by a zero charge up to the moment $t = 0^-$, constant loading from $t = 0^+$ to $t = t_1$ and a zero charge from that moment as shown in the figure 2.

For load history C2 the mathematical formulation is presented as:

$$P_{C2}\left(t\right) = Ph\left(t\right) - Ph\left(t-t_1\right). \tag{64}$$

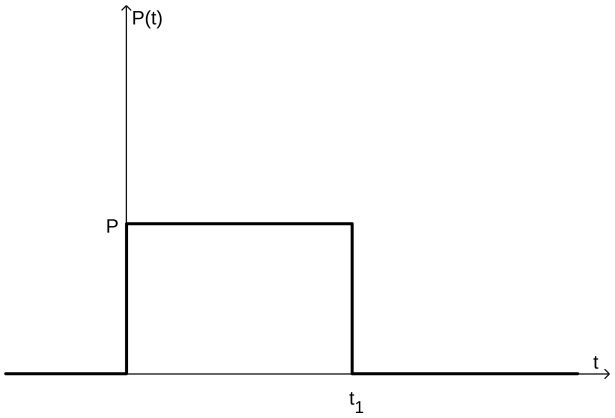

Figure 2. Load history C2

8.2 Example 01 - Traction Plate

The first example is a plate pulled in its longitudinal direction and prevented from moving in the transverse direction. (Figure 3)

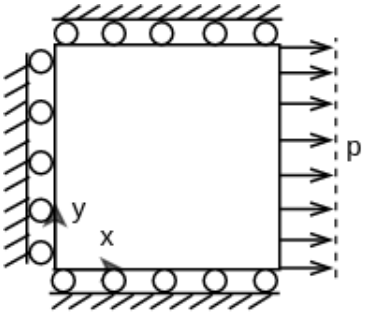

Figure 3. Traction Plate

This solid is subject to the plane stress state and is pulled by a constant load over time (p = 2MPa). The analytical solution for the creep phenomenon for x direction, displacement x (u_x) is indicated in the equation Eq. (65)

$$u_x^{C_1}(x,t) = pxh(t)\left\{\frac{3K+2q_0}{q_0(6K+q_0)} + \frac{(p_1q_0-q_1)}{2}\left[\frac{e^{-\frac{q_0}{q_1}t}}{q_0q_1} + \frac{3e^{-\frac{(6K-q_0)}{6Kp_1+q_1}t}}{(6K+q_0)(6Kp_1+q_1)}\right]\right\}, \quad (65)$$

$$\sigma_y^{C_1}(t) = ph(t)\left\{\frac{1}{6K+q_0}\left[(3K-q_0) + \frac{9K(p_1q_0-q_1)}{6Kp_1+q_1}e^{-\frac{(6K+q_0)}{6Kp_1+q_1}t}\right]\right\}. \quad (66)$$

The constants used in this problem are represented in the table. 1.

Table 1. Constants used for the example of a pull plate

K	q_0	q_1	p_1
4.17	2.50	4.00	0.80

Due to the simplicity of the problem, 09 points were used, 08 located in the boundary and 01 in domain. (Figure 4)

The total time adopted was 50s divided into parts $\Delta t = 1$s. For the historical C2, the value of t_1 equal to 25s was adopted.

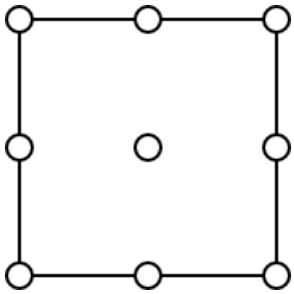

Figure 4. Domain discretization

Due to the simplicity of the problem, the results obtained by the local collocation method and local petrov galerkin method 01 were close, as an advantage of the first method due to the absence of numerical integration, reducing the computational cost of the problem. The figures 5 and 6 show the displacement u at the point with coordinates x = 2m and y = 1m, using the collocation method and the MLPG-01, respectively, for load C1.

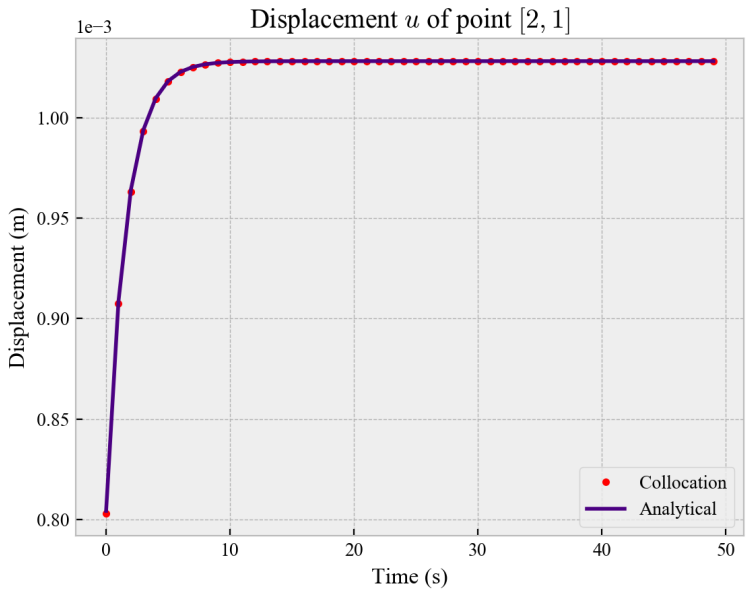

Figure 5. Collocation Method for Traction Plate Using C1 Loading

Using load history C2, the time-displacement plot for the local Petrov-Galerkin method 01 and local collocation methods were shown in the figures. 7 e 8, respectively.

Despite the greater error compared to that obtained by load C1, due to the greater complexity of load C2, the results for the two methods under study were close.

8.3 Cantilever Beam

The second example analyzed is an Cantilever Beam (see figure 9). A unitary cross-sectional thickness is considered which, allied with zero stresses in this direction, allows the simplification of the problem as a plane stress state.

The beam has constant concentrated load (P = 2N) over time. The constants used in this problem are represented in the table. 2.

The analytical solution for the creep phenomenon for direction displacement x (v_x) is indicated in the equation Eq. (67)

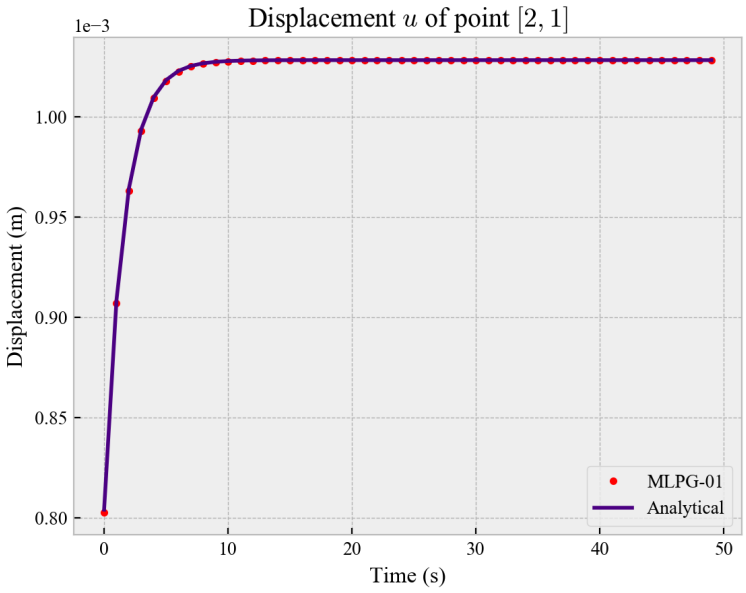

Figure 6. Local Petrov-Galerkin Method for Traction Plate Using C1 Loading

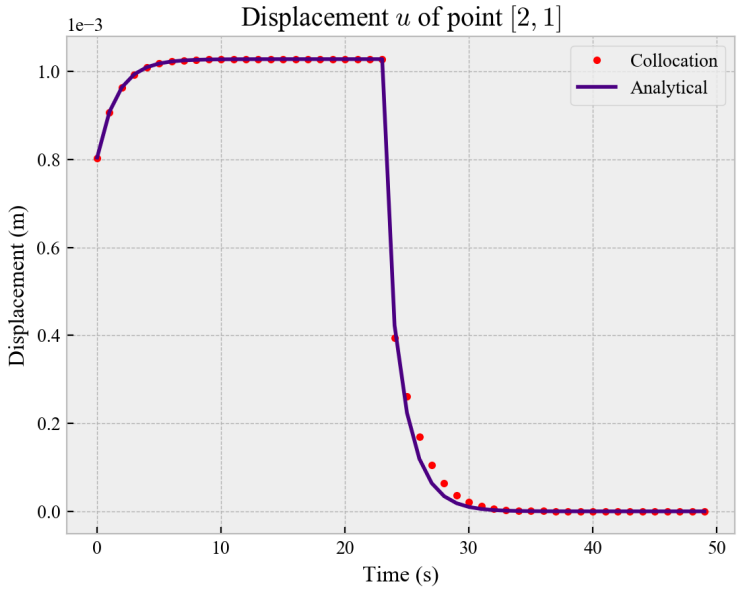

Figure 7. Collocation Method for Traction Plate Using C2 Loading

Table 2. Constants used in Cantilever Beam

L	h	K	q_0	q_1	p_1
48.00	12.00	11.67	2.50	4.00	0.80

$$v = \frac{P}{6I}\left\{\left[3y^2\left(L-x\right)+\frac{5h^2x}{4}\right]\left[\frac{3K-q_0}{9Kq_0}+\frac{\left(p_1q_0-q_1\right)}{3q_0q_1}e^{-\frac{q_0}{q_1}t}\right]\right\}$$
$$+\frac{P}{6I}\left\{\left[h^2x+x^2\left(3L-x\right)\right]\left[\frac{6K+q_0}{9Kq_0}+\frac{2\left(p_1q_0-q_1\right)}{3q_0q_1}e^{-\frac{q_0}{q_1}t}\right]\right\}. \tag{67}$$

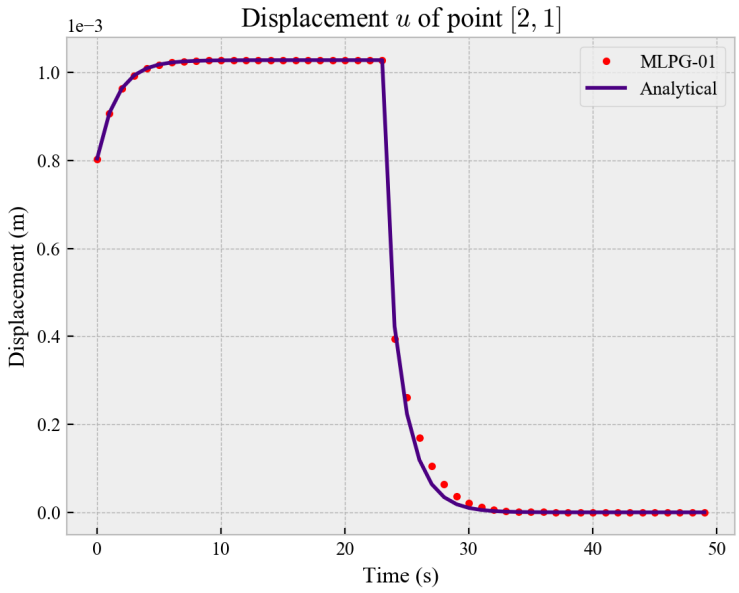

Figure 8. Local Petrov-Galerkin Method for Traction Plate Using C2 Loading

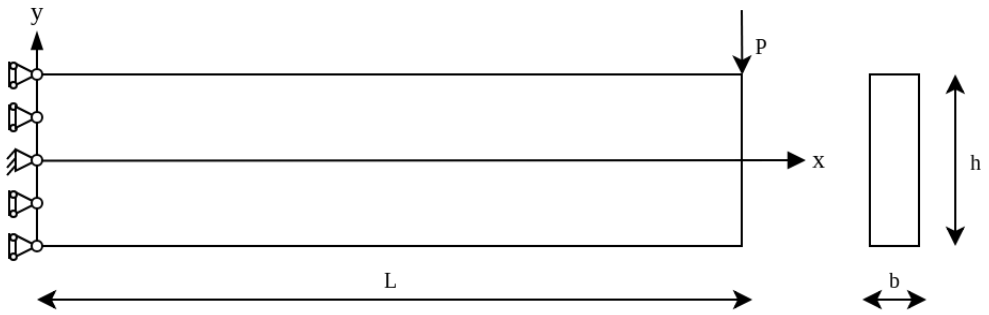

Figure 9. Cantilever Beam

Numerical solutions for the Collocation method and local Petrov-Galerkin method 01 for load C1 and node with the coordinates x = 36m and y = -3m are demonstrated by the v time-displacement graphs illustrated in the figures 10 and 11. In this case, it is possible to observe the convergence of both methods by using a sufficient number of points.

For C2 loading, it is worth noting the increase in the initial size of the radius of support by approximately 22% and the application of a regularizer method in the global matrix, due to the instabilities generated by the singularity point existing in the load, which ill-condition the matrix from the moving least squares method, and the global matrix itself. The figures 12 e 13 show the numerical results compared with the analytical solution for the collocation and MLPG-01 methods for the node with coordinates x = -3m and y = 3m.

The smallest instability from the local Petrov-Galerkin method 01, represented by the figures 12 and 13, occurs due to the reduction of the derivative order in its approximation function, resulting in smaller errors resulting from the moving least squares method.

8.4 Methods Comparison

The following are the results for the example of a Cantilever beam. In this study, for the analysis of accuracy between the methods, a discretization of 1×1 m for the two methods in order to compare the response of each method to the analytical one. The results show the advantage of the MLPG-01 over the other in terms of accuracy (Figure 14).

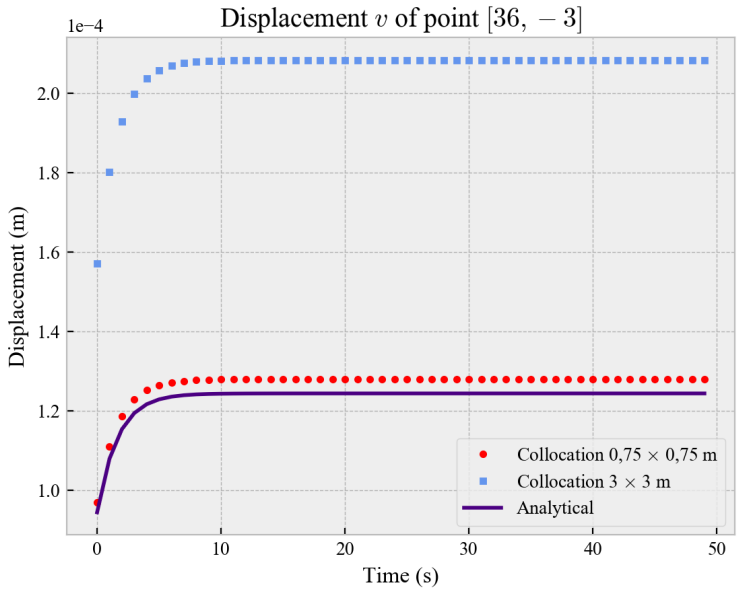

Figure 10. Collocation Method for Cantilever Beam Using C1 Loading

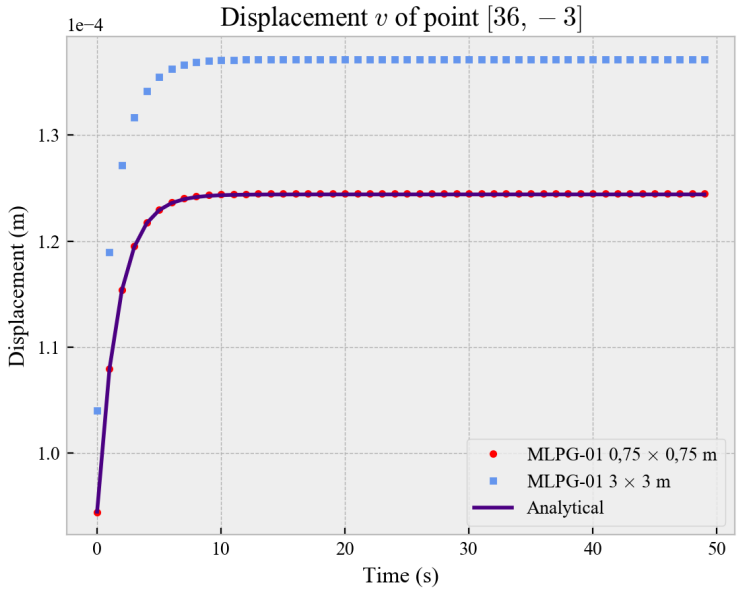

Figure 11. Local Petrov-Galerkin Method for Cantilever Beam Using C1 Loading

However, in terms of processing time, the MLPG-01 showed the worst results, having a processing time $4,5$ greater than the local collocation method.

Regarding the convergence and stability between the methods, the relative mean error for the point $[36, -3]$ with discretizations ranging from 12×3 m to $0,75 \times 0,75$ m. In the table 3 It is possible to verify the convergence of all the analyzed methods, as shown above, and also the greater stability of the local Petrov-Galerkin method 01, which did not present sudden error variations.

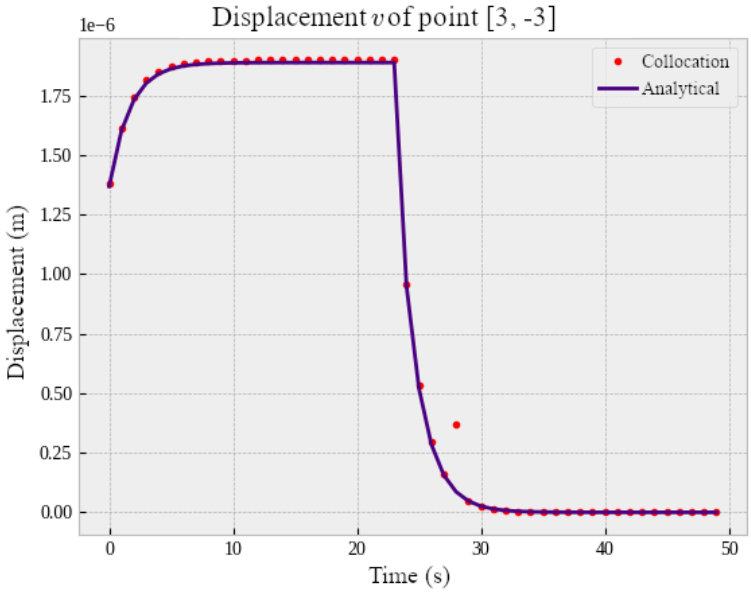

Figure 12. Collocation Method for Cantilever Beam Using C2 Loading

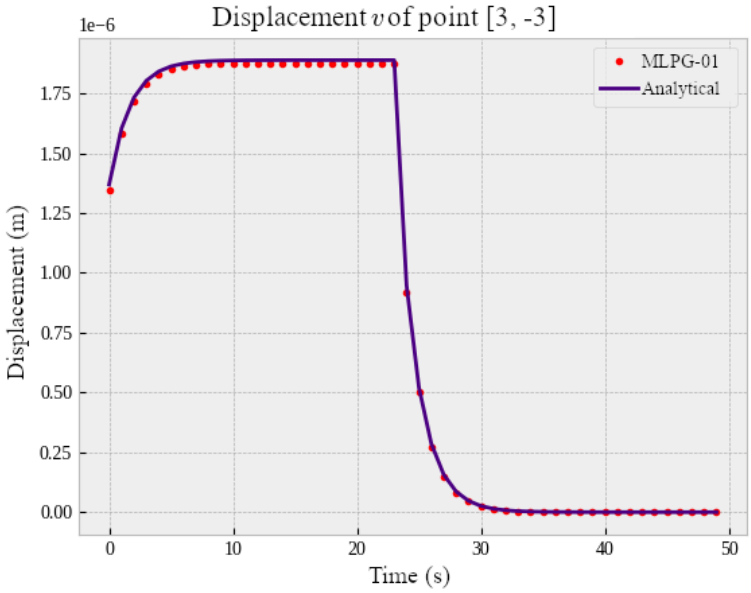

Figure 13. Local Petrov-Galerkin Method for Cantilever Beam Using C2 Loading

Table 3. Mean relative error: Cantilever Beam - v Displacement

Number of points	Collocation Method	Local Petrov-Galerkin Method
25	0.7501	1.3225
85	0.6855	0.1048
637	0.0763	0.0121
1105	0.0086	0.0008

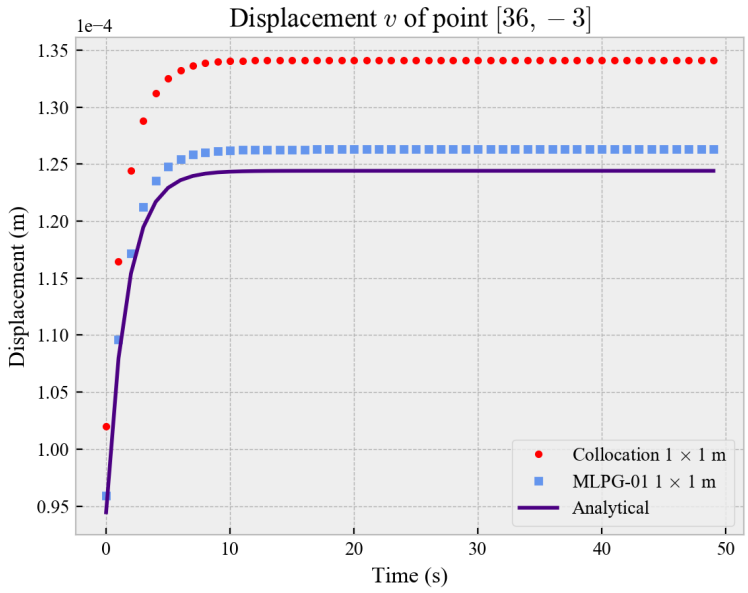

Figure 14. Comparison of methods for a Cantilever Beam Example Using C1 load (637 nodes)

8.5 Conclusion

In the present paper a methodology for numerical solution of quasi-static viscoelastic problems subjected to the plane state was developed using the local collocation method or MLPG-02 and the local Petrov-Galerkin method, alternative 01.

The choice of the support radius and the constant c of the Gaussian with radius function have significant relevance for the development of the meshless methods addressed. Inadequate values of these parameters produce poor numerical results.

The application of meshless methods, in general, obtained good results, using the Boltzmann Superposition Principle. The meshless local Petrov-Galerkin 01 method presented the best results regarding the accuracy against the others. In addition, the method demonstrated good stability, and in no case showed sudden variations of error, as depicted in the other methods. This result confirms the greater stability of weak formulation methods, as already indicated in the literature.

The local collocation method, in turn, despite the more unstable solution, regarding the processing time had great advantage to the others because it does not contain the integration phase in its formulation.

All approached methods presented adequate convergence rates, which in addition to the high accuracy rates allowed the validation of the methods for the proposed numerical problems.

Acknowledgements

The authors gratefully thanks Rio de Janeiro State University, Coordination for the Improvement of Higher Education Personnel (CAPES) and Conselho Nacional de Desenvolvimento Científico e Tecnológico (CNPq) for their support. This study was financed in part by the Coordenação de Aperfeiçoamento de Pessoal de Nível Superior- Brasil (CAPES) - Finance Code 001.

References

[1] Srivastava, A. C., S. P. K., 2011. *Engineering Mathematics : Volume Ii, Volume 2*. PHI Learning Pvt. Ltd.

[2] Belytschko, T., Krongauz, Y., Organ, D., Fleming, M., & Krys, P., 1996. Meshless methods an overview and recent developments. *Computer Methods in Applied Mechanics and Engineering*, vol. 139, pp. 3–47.

[3] Flügge, W., 1967. *Viscoelasticity*. Blaisdell Publishing Company.

[4] Atluri, S. N. & Shen, S., 2002. The Meshless Local Petrov-Galerkin (MLPG) Method: A Simple and Less-costly Alternative to the Finite Element and Boundary Element Methods. *CMES*, vol. 3, n. 1, pp. 11–51.

[5] Duarte, A. C., 1995. A review of some meshless methods to solve partial differential equations. Technical report, Texas Institute for Computational and Applied Mathematics, University of Texas at Austin,Austin, USA.

[6] Atluri, S. N. & Shen, S., 2005. The basis of meshless domain discretization: the meshless local Petrov–Galerkin (MLPG) method. *Advances in Computational Mathematics*, vol. 23, n. 1-2, pp. 73–93.

[7] Chung, T. J., 1996. *Applied Continuum Mechanics*. Cambridge University Press.

[8] Nguyen, V. P., Rabczuk, T., Bordas, S., & Duflot, M., 2008. Meshless methods: A review and computer implementation aspects. *Mathematics and Computers in Simulation*, vol. 79, pp. 763–813.

[9] Atluri, S. N. & Zhu, T., 1998a. A new meshless local Petrov–Galerkin (MLPG) approach to nonlinear problems in computational modeling and simulation. *Comput. Modeling Simulation Engrg.*, vol. 3, pp. 187–196.

[10] Atluri, S. N. & Zhu, T., 1998b. New Meshless Local Petrov-Galerkin (MLPG) approach in computational mechanics. *Computational Mechanics*, vol. 22, n. 2, pp. 117–127.

[11] Belytschko, T., Lu, Y., & Gu, L., 1994. Element-free galerkin methods. *International Journal for Numerical Methods in Engineering*, vol. 37, pp. 229–256.